Resistance to unwanted photooxidation of multi-acene molecules

Yu Yan,[#] Zachary A. Lamport,[|] Ioannis Kymissis,[|] Samuel W. Thomas III[#*]

Department of Chemistry, Tufts University, 62 Talbot Avenue, Medford, MA 02155, USA

| Department of Electrical Engineering, Columbia University, 500 W. 120th Street, New York, NY 10027 USA

ABSTRACT: Although long acenes remain a key class of π-conjugated molecules for numerous applications, photoinduced oxidation upon exposure of the acene to light, often through sensitization of $^1O_2$, is an important reaction requiring mitigation for most applications. In response to this ongoing challenge, this paper presents a series of four new diarylethynyl-substituted long acenes—three tetracenes and one anthradithiophene—in which the arylene pendants are either benzene, naphthalene, or anthracene. UV/vis and fluorescence spectroscopy reveals that the anthracene-substituted derivatives fluoresce poorly ($\Phi < 0.01$). Although all four long acenes react with $^1O_2$ at expected rates when an external photosensitizer is included, and show the expected changes in fluorescence to accompany these reactions, the anthracene-substituted derivatives resist direct photoinduced oxidation. Through a combination of mechanistic experiments, we conclude that rapid non-radiative decay of the anthracene-substituted derivatives, perhaps due to inter-arene torsions that emerge in theoretical geometry optimizations, make these compounds poor photosensitizers for $^1O_2$ or other ROS. This discovery opens new design possibilities for extended acene structures with improved photochemical stability.

INTRODUCTION

Acenes are a key class of organic molecules for a range of optical and electronic applications.[1-3] Pentacene, bis(triisopropylsilylethynyl)pentacene, and rubrene are examples of key benchmarking materials for organic field-effect transistors due to their high charge-carrier mobility in either thin films or a single-crystal devices. Their electronic structures also make acenes among the best materials for singlet fission applications in photovoltaics.[4] In addition, cycloaddition reactions, especially between anthracene moieties and reactive dieneophiles such as maleimides, are important ligation reactions for materials.[5,6,7,8]

For most applications of long acenes, such cycloadditions can be problematic, as they destroy the conjugation of the acene core and introduce bridgehead linkages. Although acene-alkyne cycloadditions or [4+4] reactions can occur,[9,10] chief among these problematic reactions is photoinduced endoperoxidation of acenes through a reactive oxygen species intermediate such as singlet oxygen or superoxide.[11,12] Typical endoperoxidation mechanisms involve photosensitized formation of either $^1O_2$, or superoxide oxidation of the acene.[13] In many cases, the acene itself acts as both the sensitizer and diene.[14]

Numerous structural modifications have emerged that can reduce the competitiveness of this oxidation.[15] Examples include: i) steric hinderance of the reactive acene core with,[16-18] ii) diethynylpentacenes that physically quench $^1O_2$;[19] iii) other directly attached pendants on pentacene, such as thiol, thioether, or open-shell substituents.[16,20] Recently, Briseno and co-workers described thiophene-substituted rubrene analogs with improved resistance to photo-oxidation attributed to rapid non-radiative decay that were unable to sensitize ROS.[21] Finally, Linker identified the reduced barriers to endoperoxide cycloreversion of ethynylated or pyridine-substituted acenes as an approach for recovering acenes after oxidation.[22,23]

Acene endoperoxidations have found important application in responsive fluorophores. Dye-anthracene conjugates can undergo fluorescence “turn-on” upon cycloaddition due to elimination of electron transfer quenching.[24,25] The commercially available probe Singlet Oxygen Sensor Green (SOSG) is an example of this approach. Our group has reported materials that contain the more reactive, longer acenes for $^1O_2$-responsive materials. These materials operate by inhibiting energy transfer from a donor chromophore to acenes, resulting in ratiometric fluorescent responses.[26] We have employed this approach in aqueous samples using conjugated polymer films,[27] acrylic polymers,[28] and conjugated polymer nanoparticles.[29,30] A persistent challenge in $^1O_2$-responsive fluorophores, however, is the proclivity of many chromophores, to sensitize ROS themselves, increasing background signal.[31] Several probes address this challenge, including the dianionic Aarhus Sensor Green of Ogilby and coworkers,[32] isobenzofuran-based probes that do not produce $^1O_2$,[33] and chemiluminescent approaches that do not require photoexcitation.[34] These probes generally use slower $^1O_2$ cycloaddition reactions than are available with longer acenes.

Inspired by recent reports of multi-acene structures for singlet fission[35-37] and thin film transistors,[38-41] we describe here a series of ethynylated long acenes with either benzene, naphthalene, or anthracene conjugated pendants. Although these molecules share the diethynylacene cores with similar reactivity, the anthracene-substituted acenes are highly stable to direct irradiation. This feature addresses the problem of unwanted ROS sensitization. We attribute this behavior to poor ROS sensitizing behavior, due to rapid non-radiative deactivation.

RESULTS AND DISCUSSION

Acene Design and Synthesis

Chart 1 shows the structures of the new acenes studied in this work. All four structures comprise a long acene core, either tetracene or anthradithiophene. Each of these four molecules has an interior fused ring with two arylethynyl substituents that terminate with triisopropylsilyl (TIPS) acetylenes. This group facilities solubility for both synthesis and analysis. The key difference between these structures are the lengths of the arene pendants, which are either benzene (**TET-1**), naphthalene (**TET-2**), or anthracene (**TET-3** and **ADT-3**), on either side of the long acene core. To compare to our previous work on simpler analogs, we also include analogous data from control compound **DE-TET** (Chart 2).[42]

Chart 1. Extended Acene Derivatives Described in this Study.

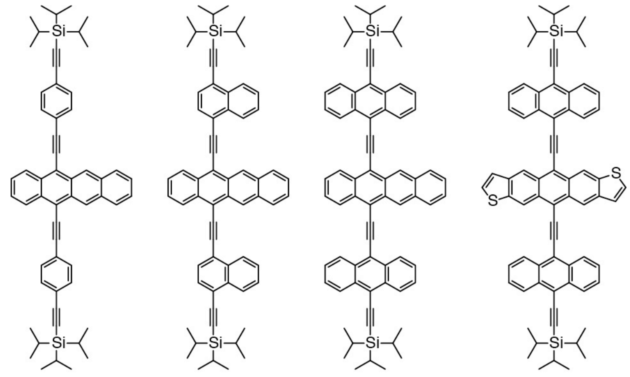

TET-1 **TET-2** **TET-3** **ADT-3**

As shown in Scheme S1 (SI), we relied on unsymmetrically substituting the pendant acene (either benzene, naphthalene, or anthracene) with an aryl iodide and a TIPS-ethynylene by selective Sonogashira coupling of the para-bromoiodide followed by lithium-bromide exchange and quenching with I_2. The resulting aryl iodides then underwent Sonogashira coupling at elevated temperatures with either diethynyltetracene or diethynylanthradithiophene, each of which was prepared from the corresponding quinones in an addition-reduction-desilylation procedure. All four final compounds were at least moderately soluble; **ADT-3** resisted dissolution the most of the four, although it was sufficiently soluble to enable characterization.

Electronic Absorbance Spectrophotometry and Density Functional Theory

Figure 1 shows the UV/vis spectra of these molecules in CH_2Cl_2 at low (10^{-5}–10^{-6} M) concentration, while **Table 1** summarizes their key spectroscopic parameters. These spectra share some common features of diethynylacenes, such as an intense and sharp transition in the UV and broad bands in the visible with some vibronic resolution. As the lengths of the acene pendants increase from benzene through anthracene, the onset of absorbance and λ_{max} of the lowest energy bands in the visible spectrum shifts to lower energy, with anthracene-conjugated **TET-3** showing λ_{max} of 590 and 620 nm. In addition, **TET-3** and **ADT-3** show distinct bands from 360-480 nm that resemble isolated diethynylanthracene chromophores. As drop-cast thin films (see Supporting Information), **TET-1** and **TET-2** show spectra that, while broadened, are consistent with those in solution. In contrast, the solid-state absorbance of both **TET-3** and **ADT-3** stretch substantially to the red, and in the case of **TET-3**, display a new intense band at 720 nm. Preliminarily, we attribute this to a combination of increased planarization and intermolecular aggregation. Although attempts to fabricate organic field-effect transistors (OFETs) in a bottom-gate, bottom-contact geometry using **TET-3** were successful,[43] the tendency of this molecule to form small needles upon deposition limited observed mobility to ~10^{-4} cm^2/Vs.

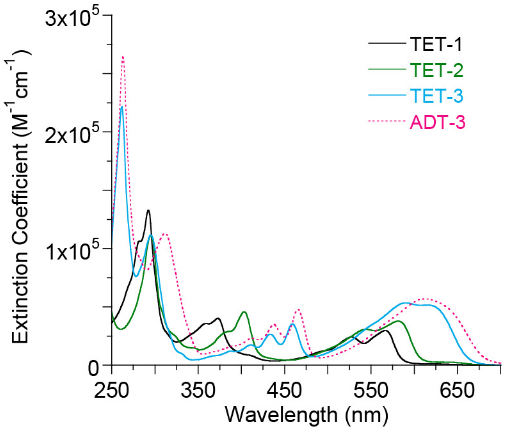

Figure 1. UV/vis absorbance spectra of acenes in CH_2Cl_2 described in this work.

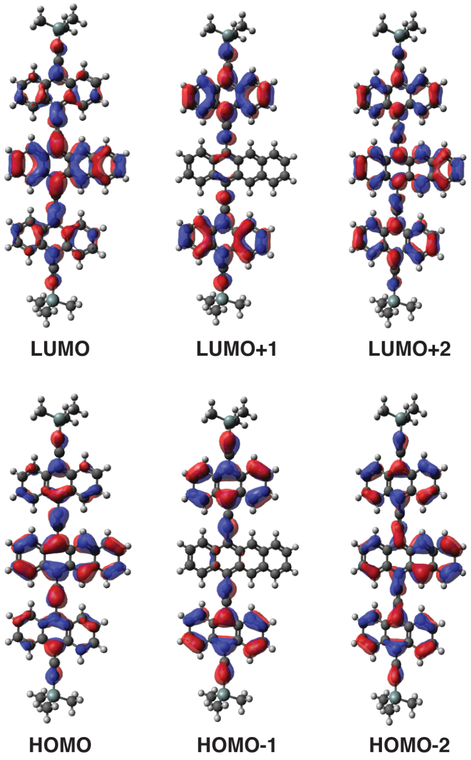

Figure 2. Molecular orbitals for **TET-3** calculated at the B3LYP/6-31G+(d,p) level. The torsional angles between the acenes are 32-35°.

We calculated the molecular orbitals and optical transitions of these molecules using density functional theory (DFT) and time-dependent DFT with the B3LYP functional and the 6-31G+(d,p) basis set. Geometry optimization at this level of theory shows torsional angles of 32-35° for **TET-3** and **ADT-3**, similar to previously reported molecules with three anthracenes connected through ethynyl linkers.[39] We attribute this twisting to steric interactions between the C-H bonds on acene rings adjacent to the ethynyl linkages—**TET-2** (20-24° torsional angles) and **TET-1** (0° torsional angles) show improved planarity between arenes. Figure 2 shows the HOMO-2 through LUMO+2 wavefunctions for **TET-3**. For all four molecules, the lowest energy transition with non-zero oscillator strength is HOMO-LUMO in nature, with the electronic density for each mostly on the central long acenes, with some occupancy along the entire π-conjugated system. As an example, **TET-3** shows two key electronic transitions calculated to result from visible light with oscillator strengths $f > 0.2$: i) 1.72 eV, purely HOMO to LUMO and ii) 2.91 eV, mostly HOMO-1 to LUMO+1, localized on the anthracene units.

Table 1. Optical and reactivity characteristics of acenes studied in this work

	λ_{onset}, nm	λ_{max}, nm	ε^{a}, M^{-1}cm^{-1}	λ_{max}(em), nm	Φ_{F}	τ_{av}	k_{rel}^{b}
TET-1	665	567*, 363, 293	29,600	581	0.33	6.3 ns	5.5
TET-2	690	581*, 403, 295	37,700	600	0.34	3.6 ns	4.1
TET-3	700	590*, 459, 262	53,400	657	< 0.001	-	4.5
ADT-3	730	612*, 466, 263	56,900	672	< 0.003	-	4.1

[a] Measured at the maximum of the longest wavelength band, indicated with an asterisk. [b] Disappearance of acene upon irradiation of MB, relative to rate measured for 9,10-diphenylanthracene (DPA, $k_{rel} = 1$) under identical conditions.

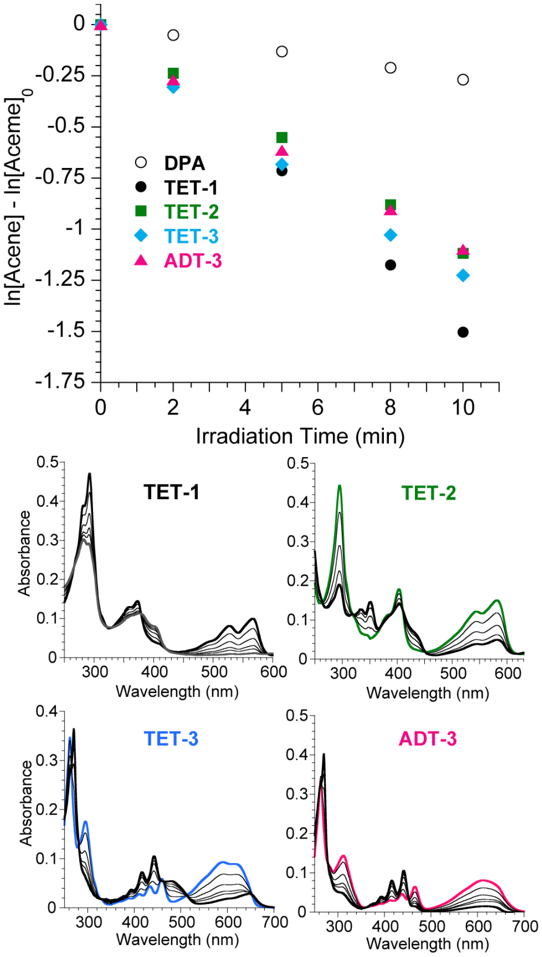

Figure 3. Pseudo first-order kinetics analysis of disappearance of acenes upon irradiation of MB. Rate constants relative to DPA (k_{rel}) for the four acenes range between 4-6. The initial absorbance spectrum of MB has been subtracted from each of these spectra.

Trends in Photo-Oxidation Reactivity with an External Photosensitizer

We began our investigation of the photochemical oxidation of these acenes by irradiating methylene blue (MB) as an external sensitizer selectively in CH_2Cl_2 using a 200W Hg/Xe lamp and a 630 nm long-pass filter to irradiate MB in the presence of each acene. We measure the concentration of the acene as a function of irradiation time using UV/vis spectrophotometry. With constant light flux and sensitizer absorbance, we assume a steady-state concentration of $^1O_2$ while irradiating, and therefore fit the resulting data to a pseudo first-order kinetic model. We also monitored the disappearance of 9,10-diphenylanthracene (DPA) in a separate experiment under identical conditions as an external standard as it resembles the reactive anthracene unit in $^1O_2$-sensitive fluorophores DPAX and Aarhus Sensor Green.[32,44]

Figure 3 summarizes the results of these experiments and analyses, which shows that the four acenes all have similar reactivities with $^1O_2$. Relative to that of DPA, these acenes react with rate constants (k_{rel}) of 4-6. This range is consistent with the reactivity of the previously reported compound from our group, **DE-TET** (Chart 2) which reacts ~5-times faster than a similar 9,10-diarylanthracene. Therefore, neither the extended arylene-ethynylene linkers nor the conjugated naphthalene or anthracene pendants noticeably impact the intrinsic reactivity of these diethynylacenes with $^1O_2$. The evolution of the optical spectra of these four acenes as they react are consistent with oxidation of the long central acene moiety, although the tetracenes retain broad absorbance between 400-500 nm. We attribute this feature to retention of the fully conjugated arylene-ethynylene linker when the tetracene is oxidized across the unsubstituted 6 and 11 positions (*vide infra*). In addition the structured absorbance of **TET-3, ADT-3** after oxidation indicates the persistence of the diethynylanthracene side groups.

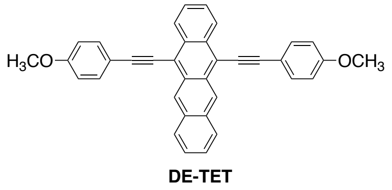

Chart 2. Structure of diethynyltetracene **DE-TET.**

NMR spectroscopy of **TET-3** upon photo-oxidation at higher acene concentration (~ 1 mM) using MB as photosensitizer provides further support for endoperoxide formation (SI). Based on the chemical shifts of the singlets associated with the hydrogen atoms on the unsubstituted 6 and 11 positions of the tetracene, we approximate a 2:1 molar ratio of the 6,11-endoperoxide to the 5,12-endoperoxide; this preference for oxidation at the non-ethynylated position of tetracene agrees with our previous work.[45]

Fluorescence Spectroscopy

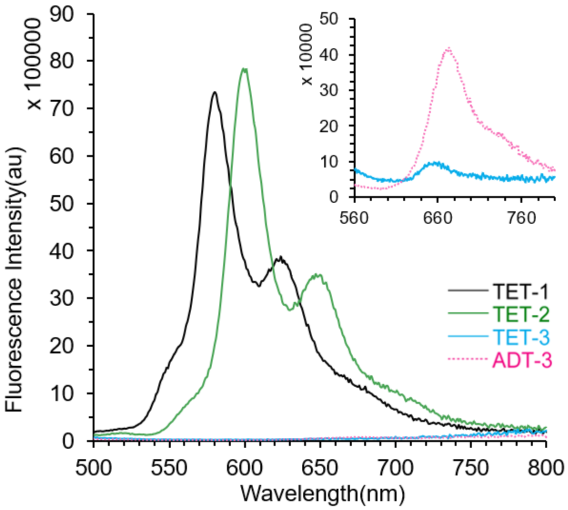

Figure 4. Normalized fluorescence spectra of acenes in CH_2Cl_2 described in this work. **TET-3** and **ADT-3** each have quantum yields of fluorescence less than 0.003. Spectra in the inset were acquired with wider slit widths (5 nm bandpass) than those in the larger plot (2 nm bandpass).

We also determined how the changes in chemical structure influence the fluorescence spectroscopy of these molecules in dilute organic solvent. Our previous work has shown that most 5,12-diethynyltetracenes and analogous diethynylanthradithiophenes have Φ_F = 0.5-0.9 and

λ_{max}(emis) = 575-590 nm;[26,42] additional phenyl substitution on the 6 and 11 positions of tetracenes shifts emission past 600 nm, with $\Phi_F > 0.6$.[46] The maximum wavelength of fluorescence for these four compounds (Figure 4) shifts with increasing conjugation of the arene pendants, from 581 nm for **TET-1**, 600 nm for **TET-2**, and greater than 650 nm for both **TET-3** and **ADT-3**. Notably, anthracene-containing **TET-3** and **ADT-3** are very weakly fluorescent ($\Phi_F < 0.003$). This observation is consistent with previously reported observations of weak fluorescence from ethynyl-bridged multi-acene structures with either two conjugated tetracenes or three conjugated anthracenes.[46,47] We attribute this quenching to rapid non-radiative decay of the excited states of **TET-3** and **ADT-3** induced by molecular motions, promoted by the steric hindrance between adjacent acenes in these molecules reflected in the geometry optimized structures. Alternative explanations we considered are inconsistent with experimental observations: intramolecular electron transfer is unlikely due to the paucity of any solvatochromic effect and the lack of donor-acceptor motifs, while intermolecular aggregation in solution is also unlikely as the shape of absorbance spectra in solution do not vary between 40 μM and 2 μM.

As shown in **Figure 5**, **TET-1** (582 nm) and **TET-2** (601 nm) show ratiometric responses to $^1O_2$: initial acene fluorescence decreases in intensity as the tetracene oxidizes, while fluorescence from the endoperoxides emerge. In contrast, the very weakly emissive **TET-3** shows a "turn-on" of fluorescence. Comparing the fluorescence of the three mixtures of oxidized tetracenes, longer pendant arenes yield bathochromically shifted final fluorescence: **TET-1** (benzene) at 425 nm, **TET-2** (naphthalene) at 452 nm, and **TET-3** (anthracene) at 537 nm. We attribute these fluorescence spectra to the tetracenes oxidized across the 6 and 11 positions, which retain a conjugated chromophore along the entire molecule. In contrast, endoperoxidation of **ADT-3** is more likely across the central anthradithiophene ring, interrupting conjugation along the arylene-ethynylene chromophore, yielding blue shifted emission (478 nm).

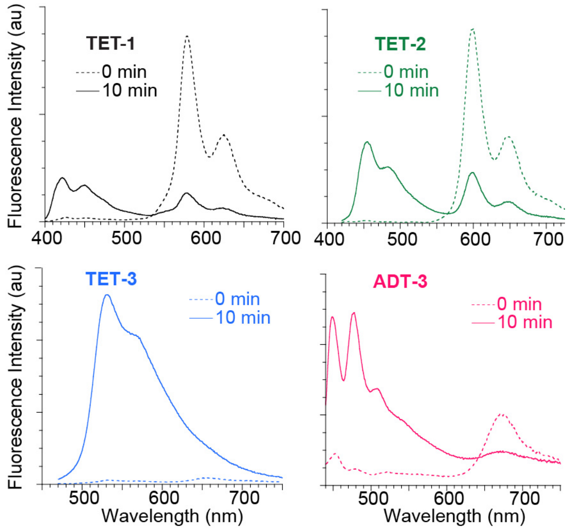

Figure 5. Fluorescent response of multi-chromophore acenes to $^1O_2$ generated through irradiation of MB in CH_2Cl_2.

Direct Irradiation Reactivity

For many applications of acenes, preventing photooxidation of acenes upon *direct irradiation* is crucial. Highly reactive acenes such as pentacene and rubrene suffer from self-sensitized oxidation, while physical quenching of $^1O_2$ bestows TIPS-pentacene with slow inherent reactivity. For fluorogenic sensing materials for $^1O_2$, direct irradiation of the fluorophore is necessary to measure luminescent response; if the fluorophore itself generates $^1O_2$ or other ROS, false positives can occur. This drawback is a reported characteristic of the commercially available Singlet Oxygen Sensor Green (SOSG).[31,32] Therefore, approaches to preventing "self-sensitization" of ROS while preserving their inherent reactivity is important for improving the performance of responsive fluorophores.

We therefore monitored the concentration of these four acenes in $CHCl_3$ in the absence of any external sensitizer, while irradiating them directly at 546 nm (12 mW/cm^2); the initial absorbance of all samples was 0.45 at 546 nm. As Figure 6 shows, fluorescent **TET-1** and **TET-2** degrade rapidly, with half-lives of 8-12 minutes. In contrast, quenched **TET-3** and **ADT-3** don not degrade after 20 minutes of irradiation. Our previous observation that the rates of reactions with $^1O_2$ for these four acenes are nearly identical makes it unlikely that physical quenching of $^1O_2$ by **TET-3** or **ADT-3** contributes to their persistence during direct irradiation. Instead, consistent with the rapid non-radiative relaxation of their excited states that we infer from Φ_F<0.003, we attribute their persistence **3** to poor photosensitization of ROS. To further support this conclusion, we compared the photosensitization performance of **TET-3** and our previously reported, highly fluorescent diethynyltetracene **DE-TET** in the oxidation of a diaryltetracene probe. As shown in the Supporting Information, irradiation of **DE-TET** completely oxidized the probe within three minutes, while irradiation of **TET-3** under otherwise identical conditions led to only 50% oxidation of the probe after thirty minutes of irradiation.

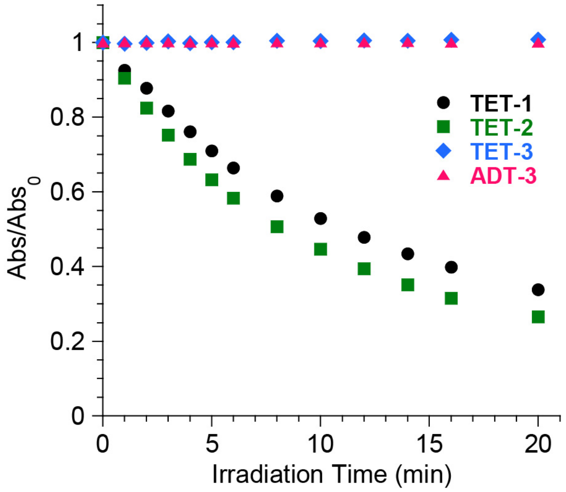

Figure 6. Photochemical bleaching of acenes during direct irradiation of each acene at 546 nm (12 mW/cm^2) in aerated $CHCl_3$.

In conclusion, this work describes the synthesis, spectroscopy, reactivity, and fluorescence response to photogenerated $^1O_2$ of four extended acenes. Our approaches for preparing these compounds are broadly applicable to others investigating multi-acene structures. Even though the aromatic pendant groups did not alter the intrinsic reactivity of these compounds with $^1O_2$ substantially, the anthracene pendants yield rapid non-radiative decay, which we attribute to steric interactions between the conjugated acenes. **TET-3** and **ADT-3** are therefore poor sensitizers, dramatically increasing their photochemical stability upon direct irradiation. Given the importance of multi-acene structures in a range of applications, we suspect that these connections between structure and reactivity will inform the work of others interested in the fundamental and applied aspects of acenes.

EXPERIMENTAL SECTION

General Information. All synthetic manipulations were performed under standard air-free conditions under an atmosphere of argon gas with magnetic stirring unless otherwise mentioned. Flash chromatography was performed using silica gel (230–400 mesh) as the stationary phase. NMR spectra were acquired on a 500 MHz spectrometer. Chemical shifts are reported relative to residual protonated solvent (7.26 ppm for $CHCl_3$ or 3.58 ppm for THF). High-resolution mass spectra (HRMS) were obtained using different ionization techniques and a peak-matching protocol to determine the mass and error range of the molecular ion.

Electronic absorbance spectra were acquired with a spectrophotometer in double-beam mode using a solvent-containing cuvette for background subtraction spectra. Fluorescence spectra were collected at a 90° angle from the incident irradiation (75W Xe lamp) and corrected for both fluctuations in the lamp intensity and the wavelength-dependent sensitivity of the photomultiplier tube detector. Fluorescence quantum yields were determined relative to coumarin 6 in ethanol.[48] Time-resolved fluorescence data were collected using a time-correlated single-photon counting instrument with a pulsed LED operating at 403 nm. Irradiation of methylene blue photosensitizer to generate $^1O_2$ was performed with a 200 W Hg/Xe lamp equipped with a condensing lens, water filter, and manual shutter, with different long pass filters. Density functional theory calculations were performed using the Gaussian 09 software package[49], with optimized geometries and FMO energies determined at the B3LYP/6-31G (d,p) level of theory using a polarizable continuum solvent model for CH_2Cl_2. The time-dependent results of these optimized geometries were calculated with the same functional and basis set, using the Tamm–Dancoff approximation.

For fabrication of transistors, highly p-doped silicon was used as the bottom-gate electrode, and 285 nm thermally grown SiO_2 served as the gate dielectric. Cr/Au (5 nm/40nm) source and drain electrodes were evaporated through a shadow mask at 0.5 Å/s and functionalized with the self-assembled monolayer (SAM) pentafluorobenzenethiol (PFBT) by vapor deposition at 70 °C for 2 hours. This SAM serves to shift the electrode work function away from the vacuum level, enhancing charge injection in p-type organic semiconductors.[50] To modify the surface energy and allow crystallites to form on the substrate, the silicon oxide layer was functionalized with trichloro(phenyl)silane by immersion in a 60 mM solution in chloroform for 1 hour, followed by immersion in fresh chloroform and a thorough rinse with 2-propanol. A 0.25 wt% solution of TET-3 in chlorobenzene was then prepared and devices were formed using solvent-assisted crystallization,[51] where the solution is drop-casted onto the patterned substrate in a covered petri dish with 100 μL chlorobenzene dispensed around the substrate. This technique creates a solvent-rich atmosphere such that the semiconductor solution evaporates more slowly, allowing for the formation of larger crystallites.[52] Electrical measurements were then taken using two Keithley 2400 source-measure units in dark at ambient atmosphere.

Synthesis

5,12-bis[2-(trimethylsilyl)ethynyl]tetracene. This reaction was executed following a reported procedure.[53] In a flame-dried 2-neck round bottom flask, trimethylsilylacetylene (0.71 mL, 490 mg, 5.0 mmol) was dissolved in 20 mL of dry diethyl ether and cooled to 0°C in an ice-water bath. *n*-Butyllithium (2.2 mL, 4.8 mmol, 2.2 M in hexanes) was added dropwise. The colorless solution was allowed to warm to room temperature and stirred for 1 h, at which time napthacenequinone (520 mg, 2.0 mmol) was added as a solid. The suspension was stirred overnight and then neutralized with 1 M HCl (aq) and $SnCl_2{\bullet}2H_2O$ (1.0 g, 4.4 mmol) was added to the mixture. After stirring for 3 h, the mixture was extracted using CH_2Cl_2 (3 x 10 mL), and the combined organic layers were dried over $MgSO_4$. The solvent was removed *in vacuo*, and the residue was purified through a plug of silica, eluted with hexanes to give 540 mg of the expected product ((65% yield) as a deep red powder .

^1H NMR (500 MHz $CDCl_3$): δ 9.20(s, 2H) 8.57-8.59 (dd , 2H), 8.08-8.10 (dd, 2H), 7.55-7.60 (dd, 2H), 7.47-7.49 (dd, 2 H), 0.54 (s, 18H). The chemical shifts are consistent with those reported in the literature.[53]

5,12-diethynyltetracene. 5,12-bis[2-(trimethylsilyl) ethynyl]tetracene (210 mg, 0.50 mmol) was dissolved in 10 mL CH_2Cl_2/methanol (1:1, v/v). To the solution, potassium carbonate (210 mg, 1.5 mmol) was added. The suspension was stirred at room temperature for 4 h. The solvent was removed, and the residue was extracted with CH_2Cl_2 (3 x 10 mL). The combined organic phase was sequentially washed with water and brine, and dried over $MgSO_4$. In syntheses of **TET-1**, **TET-2**, and **TET-3**, the crude product was used immediately after removing the solvent.

^1H NMR (500 MHz $CDCl_3$): δ 9.22 (s, 2H), 8.60-8.62 (dd, 2H), 8.08-8.10 (dd, 2H), 7.55-7.57 (dd, 2H), 7.48-7.50 (dd, 2H), 4.22 (s, 2H). $^{13}C\{^1H\}$ NMR (125 MHz $CDCl_3$): δ 132.8, 130.4, 130.2, 128.5, 127.2, 126.9, 126.2, 125.9, 90.7, 80.7.

Synthesis of TET-1

*1-bromo-4-(2-triisopropyl)ethynyl-benzene***.** Triisopropylsilylacetylene (0.22 mL, 180 mg, 1.0 mmol) of triisopropylsilyl acetylene was dissolved in 30 mL THF/triethylamine (2:1 v/v). The solution was deoxygenated with argon gas for 1 h. To another flame-dried two-neck round bottom flask, 1-iodo-4-bromobenzene (283 mg 1.0 mmol), bis(triphenylphosphine)palladium(II) dichloride (35 mg, 0.05 mmol), and copper (I) iodide (10 mg, 0.05 mmol) was added. Then, the degassed solution was transferred to the flask containing solids via cannula. The mixture was stirred overnight at room temperature. The solvent was removed *in vacuo*. The resultant solid was purified by flash column chromatography (hexanes) to yield the desired product as a colorless oil (320 mg, 95% yield). ^{1}H NMR (500 MHz CDCl$_3$): δ 7.42-7.44 (d, 2 H), 7.32-7.34 (d, 2 H), 1.09-1.12 (m, 21 H), The resonances are consistent with those reported previously in the literature.[54]

*1-iodo-4-(2-triisopropyl)ethynyl-benzene***.** In a flame-dried two-neck round bottom flask, 1-bromo-4-(2-triisopropyl)ethynyl-benzene (870 mg, 2.6 mmol) was dissolved in 10 mL of dry diethyl ether. *n*-butyllithium (1.14 mL, 2.8 mmol, 2.5 M in hexanes) was added dropwise after cooling the solution to -78 °C. The solution was stirred at -78 °C for 1 h. I$_2$ was added as a solid (857 mg, 3.4 mmol) and the mixture was allowed to warm up to ambient temperature. The reaction was then stirred for 8 h followed by quenching with 10 mL saturated ammonium chloride solution. The mixture was then extracted with CH$_2$Cl$_2$ and dried over MgSO$_4$. The crude product (870 mg, 87% yield) was directly used after removing the solvent without any further purification.

5,12-bis[((4-triisopropylethynyl)phenyl)ethynyl]tetracene (**TET-1**). In a round bottom flask, 1-iodo-4-(2-triisopropyl)ethynyl-benzene (670 mg, 1.7 mmol) was dissolved in 9 mL toluene/diisopropylamine (2:1 v/v). The solution was deoxygenaged by bubbling with argon for 1 h. To another flame dried two-neck round bottom flask equipped with a condenser, 5,12-diethynyltetracene (180 mg, 0.63 mmol), Cl$_2$Pd(PPh$_3$)$_2$ (30 mg, 0.04 mmol), and CuI (10 mg, 0.05 mmol) was added. The degassed solution was then transferred to the flask via a syringe. The mixture was then stirred at 80 °C in an oil bath for 36 h. The solvent was removed *in vacuo*, and the residue was purified via flash column chromatography (CH$_2$Cl$_2$/hexanes 1:1 v/v). The crude product was recrystallized from CHCl$_3$/MeOH to yield **TET-1** (150 mg, 30% yield) as a purple solid.

^{1}H NMR (500 MHz CDCl$_3$): δ 1.17-1.18 (m, 42 H), 7.49-7.51 (dd, 2 H), 7.58-7.59 (m, 6 H), 7.60 (d, 4H), 8.11-8.12 (dd, 2H), 8.64-8.65 (dd, 2H), 9.25 (s, 2H). ^{13}C{^{1}H} NMR (125 MHz CDCl$_3$): δ 132.4, 132.2, 131.5, 129.9, 128.6, 127.4, 126.8, 126.2, 126.1, 123.9, 123.3, 118.3, 106.7, 103.2, 93.4, 89.0, 18.7, 11.4. HRMS (TOF, EI): m/z calcd for $C_{56}H_{60}Si_2$ (M$^+$) 788.4234, found 788.4212.

Synthesis of TET-2

*1-bromo-4-(2-triisopropyl)ethynyl-naphthalene***.** A flame-dried round bottom flask was charged with 1-iodo-4-bromonaphthalene (1.2 g, 3.7 mmol) and 30 mL of degassed THF/NEt$_3$ (2:1 v/v). Pd(PPh$_3$)$_2$Cl$_2$ (100 mg, 0.14 mmol) and CuI (0.2 mmol, 40 mg) was added to the solution. With a syringe, triisopropylsilylacetylene (0.82 mL, 3.7 mmol) was added to the solution. The reaction was stirred overnight before purification by elution through a plug of silica with hexanes. After removing the solvent under vacuum, 1.25 g of the desired product was obtained as a pale-yellow oil. (88% yield).

^{1}H NMR (500 MHz CDCl$_3$): δ 8.40-8.41 (m, 1H), 8.24-8.26 (m, 1H), 7.72-7.73 (d, 1H), 7.62-7.65 (m, 2 H), 7.54-7.56 (d, 1 H), 1.19-1.20 (m, 21 H),

^{13}C{^{1}H} NMR (125 MHz CDCl$_3$): δ 134.5, 132.8, 131.7, 130.9, 129.3, 127.7, 127.5, 126.8, 123.6, 121.3, 104.1, 97.3, 18.8 11.4.

1-iodo-4-(2-triisopropyl)ethynyl-naphthalene. In a flame dried round bottom flask, 1-bromo-4-(2-triisopropyl)ethynyl-naphthalene (1.25 g, 3.3 mmol) was dissolved in 10 mL of dry THF. The solution was cooled to -78 °C using an acetone/dry ice bath. With a syringe, *n*-butylithium solution (2.0 mL, 5.0 mmol, 2.5 M in hexanes) was added dropwise. The solution was stirred at -78 °C for 1 h, and then I$_2$ (1.5 g, 6 mmol) was added as a solid. The reaction was stirred overnight, and then quenched with aqueous NaS$_2$O$_3$. The mixture was extracted with CH$_2$Cl$_2$ three times, and the combined organic layers were dried over MgSO$_4$. Then, the solvent was removed *in vacuo* to yield 1.38 g yellow oil. This crude product was directly used in the next step without further purification (96% yield).

5,12-bis[((4-triisopropylethynyl)naphthyl)ethynyl]tetracene (**TET-2**). A round bottom flask was charged with a solution of 1-iodo-4-(2-triisopropyl)ethynyl-naphthalene (1.0 g, 2.3 mmol) dissolved in 14 mL of a toluene/diisopropylamine (4:3 v/v) mixture. The solution was then deoxygenated by bubbling with argon for 1 h. This solution was transferred by cannula into a flamed dried round bottom flask containing compound **8** (280 mg, 1.0 mmol), Pd(PPh$_3$)$_2$Cl$_2$ (35 mg, 0.05 mmol), and CuI (10 mg, 0.05 mmol). The reaction was heated to 80 °C in an oil bath and stirred for 20 h. The mixture was first purified by flash column chromatography (gradient elution 1:4 CH$_2$Cl$_2$/hexane to 100% CH$_2$Cl$_2$). Finally, 530 mg of pure **TET-2** was isolated by recrystallization from chloroform/methanol as a purple solid (60% yield).

^{1}H NMR (500 MHz CDCl$_3$): δ 9.39 (s, 2H), 8.76-8.80 (m, 4 H), 8.51-8.53 (m, 2 H), 8.08-8.10 (dd, 2 H), 7.99-8.00 (d, 2H), 7.81-7.83 (d, 2H), 7.71-7.76 (m, 6H), 7.62-7.64 (dd, 2 H), 7.49-7.51 (dd, 2 H), 1.24-1.28 (m, 42 H). ^{13}C{^{1}H} NMR (125 MHz CDCl$_3$): δ 133.0, 132.4, 132.3, 130.5, 130.1, 130.0, 128.6, 127.53, 127.50, 126.9, 126.8, 126.2, 122.3, 121.8, 118.6, 104.8, 101.8, 98.5, 93.7, 18.8, 11.5. HRMS (MALDI, matrix: DCTB): m/z calcd for $C_{64}H_{64}Si_2$ (M$^+$) 888.4547, found 888.4537.

Synthesis of TET-3

*9-iodo-10-bromo-anthracene***.** In a flame-dried round bottom flask, 9,10-dibromoanthracene (1.0 g, 3.0 mmol) was added to 30 mL of dry THF and cooled to -78 °C. To the suspension, *n*-butyllithium (1.3 mL, 3.3 mmol, 2.5 M in hexanes) was added dropwise. The resulting solution was allowed to warm to room temperature and stirred for another 3 hours. The flask was cooled to -78°C again followed by the addition of 1.0 g of I$_2$ (3.9 mmol). After stirring at room temperature for 20 h, the solution was concentrated *in vacuo* to approximately 10% of its original volume. Sodium thiosulfate aqueous solution (20 mL, 20% w/v) was mixed into the residue, and the resulting precipitate was collected by vacuum filtration to afford the desired product as needle-shaped yellow crystals (1.04 g, 91% yield)

^{1}H NMR (500 MHz $CDCl_3$): δ 8.56-8.58 (m, 4 H), 7.61-7.63 (m, 4H). The chemical shifts are consistent with those reported previously in the literature.[55]

*9-bromo-10-(2-triisopropyl)ethynyl-anthracene***.** A flame-dried round bottom flask was charged with a solution of 9-iodo-10-bromo-anthracene (1.04 g, 2.7 mmol) dissolved in 30 mL of a degassed THF/ NEt_3 (2:1, v/v) mixture. $Pd(PPh_3)_2Cl_2$ (98 mg, 0.14 mmol) and CuI (26 mg, 0.14 mmol) were added to the solution. With a syringe, triisopropylsilyl acetylene (0.61 mL, 2.7 mmol) was added to the solution. The mixture was stirred overnight at ambient temperature. The solvent was then removed *in vacuo* and the residue was purified by flash column chromatography (hexanes) to afford 1.10 g of the desired product as a pale yellow oil (93% yield).

^{1}H NMR (500 MHz $CDCl_3$): δ 8.54-8.68 (m, 4H), 7.60-7.64 (m, 4H), 1.25-1.30 (m, 21 H). The resonances are consistent with those reported previously.[56]

9-iodo-10-(2-triisopropyl)ethynyl-anthracene. In a flame-dried round bottom flask, 9-bromo-10-(2-triisopropyl)ethynyl-anthracene (600 mg, 1.4 mmol) was dissolved in 10 mL of dry diethyl ether. The solution was then cooled to -78°C. *n*-butyllithium (1.1 mL, 2.1 mmol, 2.2 M in hexanes) was added dropwise to the solution. The mixture was stirred for 1 h at -78°C, after which solid I_2 (630 mg, 2.5 mmol) was added to the mixture, and the reaction was allowed to warm to room temperature and stirred overnight. After quenching by adding sodium thiosulfate aqueous solution (20% w/v), the mixture was extracted with diethyl ether three times. The combined organic layers were dried over $MgSO_4$ and the solvent was removed under vacuum to afford the desired product as a red oil, (626 mg, 93% yield) which was used for the next step without further purification.

5,12-bis[((10-triisopropylethynyl)anthracenyl)ethynyl]tetracene (**TET-3**). A round bottom flask was charged with 9-iodo-10-(2-triisopropyl)ethynyl-anthracene (490 mg, 1.0 mmol) dissolved in 5 mL of a toluene/diisopropylamine mixture (3:2 v/v). The solution was then deoxygenated by bubbling with argon for 1 h. To a flame-dried round bottom flask, compound **8** (130 mg, 0.5 mmol), Pd(PPh3)$_2$Cl$_2$ (14 mg, 0.02 mmol) and CuI (10 mg, 0.05 mmol) were added as solids. The degassed solution was transferred into the flask containing solids using a cannula.. After stirring in the dark for 24 hours at 80 °C in an oil bath, the solvent was removed *in vacuo*. The residue was passed through a plug of silica with CH_2Cl_2 to remove highly polar impurities. The product was then recrystallized from acetone to yield 140 mg of **TET-3** as a blue solid (28% yield).

^{1}H NMR (500 MHz THF-*d8*): δ 9.48 (s, 2H), 8.99-9.01 (dd, 4H), 8.84-8.86 (dd, 2H), 8.70-8.72 (dd, 4H), 8.05-8.07 (dd, 2H), 7.66-7.71 (m, 10 H), 7.49-7.51 (dd, 2 H), 1.34-1.35 (m, 42 H). ^{13}C{^{1}H} NMR (125 MHz THF-*d8*): δ 11.6, 18.4, 100.4,100.8, 103.7, 105.0, 118.6, 118.8, 126.1, 126.3, 127.0, 127.07, 127.10, 127.14, 127.3, 128.4, 129.8, 132.1, 132.3, 132.4, 132.5. HRMS (MALDI matrix: DCTB): m/z calcd for $C_{72}H_{68}Si_2$ (M^+) 988.4860, found 988.4817.

Synthesis of ADT-3

Anthradithiophene-5,11-dione. 1,4-cyclohexanedione (0.84 g, 7.5 mmol) was added to a solution of 2,3-thiophene dicarbaldehyde (2.1 g, 15 mmol) in 100 mL ethanol. 6 mL of 15% (w/v) KOH aqueous solution was then added dropwise. The reaction was stirred at ambient temperature for four hours. The resulting precipitate was collected by vacuum filtration and washed with ethanol to obtain the product as a yellow solid. (2.4 g, 99% yield), which was used directly without any purification.

5,11-bis[2-(trimethylsilyl)ethynyl]-anthradithiophene. In a flame-dried round bottom flask, triisopropylsilylacetylene (1.1 mL, 5.0 mmol) was dissolved in 20 mL of dry diethyl ether and cooled to 0 °C. A solution of *n*-BuLi (5 mmol, 2.0 mL 2.5 M in hexanes) was added dropwise. The mixture was stirred at 0 °C for 30 minutes and stirred at room temperature for another hour. Then, anthradithiophene-5,11-dione (640 mg, 2.0 mmol) was added as a solid. The reaction was stirred at room temperature overnight. The pH of the reaction was tuned to approximately 7 using a 0.1 M HCl aqueous solution, and then 1.0 g of $SnCl_2·2H_2O$ was added to the mixture. This mixture was stirred in the dark for 3 hours. The mixture was extracted with diethyl ether 3 times and the combined organic phases were dried over $MgSO_4$. The crude product was purified using column chromatography (hexanes) to obtain the desired product (850 mg, 60% yield).

^{1}H NMR (300 MHz, $CDCl_3$): δ 9.20 (s, 2H), 9.16 (s, 2H), 7.55-7.56 (d, 2H), 7.43-7.44 (d, 2H), 1.32-1.38 (m, 42H), These resonances are consistent with those reported in the literature.[10]

5,11-diethynylanthradithiophene. In a round bottom flask, 5,11-bis[2-(trimethylsilyl)ethynyl]-anthradithiophene (130 mg 0.20 mmol) was dissolved in 5 mL of THF and cooled to -78 °C. 2.0 mL of TBAF solution (1 M in THF) was added dropwise. In the dark, the reaction was stirred for 5 min at -78 °C and stirred for another hour at room temperature. After quenching the reaction with 10 mL of water, the precipitate was filtered and washed with water and cold methanol to afford the desired product as a red solid. (340 mg, 83% yield)

^{1}H NMR (300 MHz $CDCl_3$): δ = 9.19 (s, 2H), 9.12 (s, 2H), 7.56-7.58 (d, 2H), 7.48-7.49 (d, 2H). 4.24-4.29 (m, 2H). The solubility of this compound is very low in solvents for NMR spectroscopy. Thus, the ^{13}C NMR spectrum could not be obtained with high quality.

5,11-Bis[((10-triisopropylethynyl)anthracenyl)ethynyl]anthradithiophene (**ADT-3**). In a round bottom flask, 9-iodo-10-(2-triisopropyl)ethynyl-anthracene (1.20 g, 2.5 mmol) was dissolved in 15 mL of THF/diisopropylamine (2:1 v/v). The solution was then deoxygenated by bubbling with argon gas for 1 h. In another flame-dried flask, of 5,11-diethynylanthradithiophene (340 mg, 1.0 mmol), Pd(PPh3)$_2$Cl$_2$ (35 mg, 0.05 mmol), and CuI (10 mg, 0.05 mmol) were added as solids. The degassed solution was then added to the flask with solids using a cannula. The reaction was stirred at 80 °C in an oil bath for 24 hours. After removal of solvent *in vacuo*, the residue was passed through a plug of silica with CH_2Cl_2 eluent. The product

was recrystallized from acetone twice and then chloroform/methanol twice to yield **ADT-3** as a dark green solid. (250 mg, 25% yield).
^{1}H NMR (500 MHz THF-*d8*): δ 9.00-9.07 (m, 4H), 8.73-8.74 (m, 4H), 8.58-8.60 (m, 4H), 7.60 (m, 2H), 7.56 (m, 4H), 7.25 (m, 4 H), 6.92 (m, 2 H), 1.38-1.4 (m, 42 H). HRMS (MALDI matrix: DCTB): m/z calcd for $C_{72}H_{66}S_2Si_2$ (M^+) 1050.4144, found 1050.4104. The product is a mixture of slightly soluble trans-/cis- isomers, so the multiplicity of signals cannot be distinguished. However, the structure can be confirmed by the HRMS and 2D-NMR. In addition, the solubility of **ADT-3** is very low in solvents for NMR spectroscopy. Thus, the ^{13}C NMR spectrum cannot be obtained with high quality.

ASSOCIATED CONTENT

Supporting Information

The Supporting Information is available free of charge on the ACS Publications website.

NMR spectra of new compounds, spectroscopic and reactivity experiments. (PDF)

AUTHOR INFORMATION

Corresponding Author

* sam.thomas@tufts.edu

ACKNOWLEDGMENT

This work was supported by the National Science Foundation (CHE-1609146). Z. L. thanks Corning and the NSF under STTR 1914013 for financial support.

REFERENCES

1. Anthony, J. E. The Larger Acenes: Versatile Organic Semiconductors. *Angew. Chem. Int. Ed.* **2008,** *47,* 452-483.
2. Wang, C.; Dong, H.; Hu, W.; Liu, Y.; Zhu, D. Semiconducting π-Conjugated Systems in Field-Effect Transistors: A Material Odyssey of Organic Electronics. *Chem. Rev.* **2012,** *112,* 2208-2267.
3. Wang, C.; Dong, H.; Jiang, L.; Hu, W. Organic Semiconductor Crystals. *Chem. Soc. Rev.* **2018,** *47,* 422-500.
4. Zimmerman, P. M.; Bell, F.; Casanova, D.; Head-Gordon, M. Mechanism for Singlet Fission in Pentacene and Tetracene: From Single Exciton to Two Triplets. *J. Am. Chem. So.* **2011,** *133,* 19944-19952.
5. Van Damme, J.; Du Prez, F. Anthracene-Containing Polymers toward High-End Applications. *Prog. Polym. Sci.* **2018,** *82,* 92-119.
6. Tasdelen, M. A. Diels–Alder "Click" Reactions: Recent Applications in Polymer and Material Science. *Polym. Chem.* **2011,** *2,* 2133-2145.
7. Kabb, C. P.; O'Bryan, C. S.; Morley, C. D.; Angelini, T. E.; Sumerlin, B. S. Anthracene-Based Mechanophores for Compression-Activated Fluorescence in Polymeric Networks. *Chem. Sci.* **2019,** *10,* 7702-7708.
8. Frank, P. G.; Tuten, B. T.; Prasher, A.; Chao, D.; Berda, E. B. Intra-Chain Photodimerization of Pendant Anthracene Units as an Efficient Route to Single-Chain Nanoparticle Fabrication. *Macromol. Rapid Commun.* **2014,** *35,* 249-253.
9. Purushothaman, B.; Parkin, S. R.; Anthony, J. E. Synthesis and Stability of Soluble Hexacenes. *Org. Lett.* **2010,** *12,* 2060-2063.
10. Payne, M. M.; Odom, S. A.; Parkin, S. R.; Anthony, J. E. Stable, Crystalline Acenedithiophenes with up to Seven Linearly Fused Rings. *Org. Lett.* **2004,** *6,* 3325-3328.
11. Aubry, J.-M.; Pierlot, C.; Rigaudy, J.; Schmidt, R. Reversible Binding of Oxygen to Aromatic Compounds. *Acc. Chem. Res.* **2003,** *36,* 668-675.
12. Maliakal, A.; Raghavachari, K.; Katz, H.; Chandross, E.; Siegrist, T. Photochemical Stability of Pentacene and a Substituted Pentacene in Solution and in Thin Films. *Chem. Mater.* **2004,** *16,* 4980-4986.
13. Reddy, A. R.; Bendikov, M. Diels–Alder Reaction of Acenes with Singlet and Triplet Oxygen – Theoretical Study of Two-State Reactivity. *Chem. Commun.* **2006,** 1179-1181.
14. Liu, K.; Lalancette, R. A.; Jäkle, F. Tuning the Structure and Electronic Properties of B–N Fused Dipyridylanthracene and Implications on the Self-Sensitized Reactivity with Singlet Oxygen. *J. Am. Chem. Soc.* **2019,** *141,* 7453-7462.
15. Shi, X.; Chi, C. Different Strategies for the Stabilization of Acenes and Acene Analogues. *Chem. Record* **2016,** *16,* 1690-1700.
16. Kaur, I.; Jia, W.; Kopreski, R. P.; Selvarasah, S.; Dokmeci, M. R.; Pramanik, C.; McGruer, N. E.; Miller, G. P. Substituent Effects in Pentacenes: Gaining Control over HOMO–LUMO Gaps and Photooxidative Resistances. *J. Am. Chem. Soc.* **2008,** *130,* 16274-16286.
17. Zhang, J.; Pawle, R. H.; Haas, T. E.; Thomas Iii, S. W. Combining Electronic and Steric Effects for Highly Stable Unsymmetric Pentacenes. *Chem. Eur. J.* **2014,** *20,* 5880-5884.
18. Baral, R. N.; Thomas, S. W. Steric and Electronic Substituent Effects Influencing Regioselectivity of Tetracene Endoperoxidation. *J. Org. Chem.* **2015,** *80,* 11086-11091.
19. Fudickar, W.; Linker, T. Why Triple Bonds Protect Acenes from Oxidation and Decomposition. *J. Am Chem. Soc.* **2012,** *134,* 15071-15082.
20. Shimizu, A.; Ito, A.; Teki, Y. Photostability Enhancement of the Pentacene Derivative Having Two Nitronyl Nitroxide Radical Substituents. *Chem. Commun.* **2016,** *52,* 2889-2892.
21. Ly, J.; Martin, K.; Thomas, S.; Yamashita, M.; Yu, B.; Pointer, C. A.; Yamada, H.; Carter, K. R.; Parkin, S.; Zhang, L.; Bredas, J.-L.; Young, E. R.; Briseno, A. L. Short Excited-State Lifetimes Enable Photo-Oxidatively Stable Rubrene Derivatives. *J. Phys. Chem. A* **2019,** *123,* 7558-7566.
22. Fudickar, W.; Linker, T. Release of Singlet Oxygen from Aromatic Endoperoxides by Chemical Triggers. *Angew. Chem. Int. Ed.* **2018,** *57,* 12971-12975.
23. Fudickar, W.; Linker, T. Reversible Photooxygenation of Alkynylanthracenes: Chemical Generation of Singlet Oxygen under Very Mild Conditions. *Chem. Eur. J.* **2011,** *17,* 13661-13664.
24. Tanaka, K.; Miura, T.; Umezawa, N.; Urano, Y.; Kikuchi, K.; Higuchi, T.; Nagano, T. Rational Design of Fluorescein-Based Fluorescence Probes. Mechanism-Based Design of a Maximum Fluorescence Probe for Singlet Oxygen. *J. Am. Chem. Soc.* **2001,** *123,* 2530-2536.
25. You, Y. Chemical Tools for the Generation and Detection of Singlet Oxygen. *Org. Biomol. Chem.* **2018,** *16,* 4044-4060.
26. Altınok, E.; Smith, Z. C.; Thomas, S. W. Two-Dimensional, Acene-Containing Conjugated Polymers That Show Ratiometric Fluorescent Response to Singlet Oxygen. *Macromolecules* **2015,** *48,* 6825-6831.
27. Koylu, D.; Sarrafpour, S.; Zhang, J.; Ramjattan, S.; Panzer, M. J.; Thomas, S. W. Acene-Doped Polymer Films: Singlet Oxygen Dosimetry and Protein Sensing. *Chem. Commun.* **2012,** *48,* 9489-9491.

28. Altinok, E.; Frausto, F.; Thomas, S. W. Water-Soluble Fluorescent Polymers That Respond to Singlet Oxygen. *J. Polym. Sci. A Polym. Chem.* **2016,** *54,* 2526-2535.

29. Frausto, F.; Thomas, S. W. Tuning the Key Properties of Singlet Oxygen-Responsive Acene-Doped Conjugated Polymer Nanoparticles. *ChemPhotoChem* **2018,** *2,* 632-639.

30. Frausto, F.; Thomas, S. W. Ratiometric Singlet Oxygen Detection in Water Using Acene-Doped Conjugated Polymer Nanoparticles. *ACS Appl. Mater. Interf.* **2017,** *9,* 15768-15775.

31. Kim, S.; Fujitsuka, M.; Majima, T. Photochemistry of Singlet Oxygen Sensor Green. *J. Phys. Chem. B* **2013,** *117,* 13985-13992.

32. Pedersen, S. K.; Holmehave, J.; Blaikie, F. H.; Gollmer, A.; Breitenbach, T.; Jensen, H. H.; Ogilby, P. R. Aarhus Sensor Green: A Fluorescent Probe for Singlet Oxygen. *J. Org. Chem.* **2014,** *79,* 3079-3087.

33. Song, D.; Cho, S.; Han, Y.; You, Y.; Nam, W. Ratiometric Fluorescent Probes for Detection of Intracellular Singlet Oxygen. *Org. Lett.* **2013,** *15,* 3582-3585.

34. Hananya, N.; Green, O.; Blau, R.; Satchi-Fainaro, R.; Shabat, D. A Highly Efficient Chemiluminescence Probe for the Detection of Singlet Oxygen in Living Cells. *Angew. Chem. Int. Ed.* **2017,** *56,* 11793-11796.

35. Fuemmeler, E. G.; Sanders, S. N.; Pun, A. B.; Kumarasamy, E.; Zeng, T.; Miyata, K.; Steigerwald, M. L.; Zhu, X. Y.; Sfeir, M. Y.; Campos, L. M.; Ananth, N. A Direct Mechanism of Ultrafast Intramolecular Singlet Fission in Pentacene Dimers. *ACS Central Sci.* **2016,** *2,* 316-324.

36. Korovina, N. V.; Das, S.; Nett, Z.; Feng, X.; Joy, J.; Haiges, R.; Krylov, A. I.; Bradforth, S. E.; Thompson, M. E. Singlet Fission in a Covalently Linked Cofacial Alkynyltetracene Dimer. *J. Am. Chem. Soc.* **2016,** *138,* 617-627.

37. Korovina, N. V.; Joy, J.; Feng, X.; Feltenberger, C.; Krylov, A. I.; Bradforth, S. E.; Thompson, M. E. Linker-Dependent Singlet Fission in Tetracene Dimers. *J. Am. Chem. Soc.* **2018,** *140,* 10179-10190.

38. Dell'Aquila, A.; Marinelli, F.; Tey, J.; Keg, P.; Lam, Y.-M.; Kapitanchuk, O. L.; Mastrorilli, P.; Nobile, C. F.; Cosma, P.; Marchenko, A.; Fichou, D.; Mhaisalkar, S. G.; Suranna, G. P.; Torsi, L. 9,10-Ter-Anthrylene-Ethynylene: A New Molecular Architecture for Solution Processed Anthracene-Based Thin Film Transistors. *J. Mater. Chem.* **2008,** *18,* 786-791.

39. Keg, P.; Dell'Aquila, A.; Marinelli, F.; Kapitanchuk, O. L.; Fichou, D.; Mastrorilli, P.; Romanazzi, G.; Suranna, G. P.; Torsi, L.; Lam, Y. M.; Mhaisalkar, S. G. Solution Processable Ter-Anthrylene-Ethynylenes Semiconductors: Thin Film Transistor Properties and STM Study on Hopg and Au(111). *J. Mater. Chem.* **2010,** *20,* 2448-2456.

40. Romanazzi, G.; Dell'Aquila, A.; Suranna, G. P.; Marinelli, F.; Cotrone, S.; Altamura, D.; Giannini, C.; Torsi, L.; Mastrorilli, P. Solution Processed Ter-Anthrylene-Ethynylenes for Annealing-Activated Organic Field-Effect Transistors: A Structure–Performance Correlation Study. *J. Mater. Chem.* **2011,** *21,* 15186-15189.

41. Kawano, K.; Hayashi, H.; Yoshimoto, S.; Aratani, N.; Suzuki, M.; Yoshinobu, J.; Yamada, H. An Ethynylene-Bridged Pentacene Dimer: Two-Step Synthesis and Charge-Transport Properties. *Chem. Eur. J.* **2018,** *24,* 14916-14920.

42. Zhang, J.; Smith, Z. C.; Thomas, S. W. Electronic Effects of Ring Fusion and Alkyne Substitution on Acene Properties and Reactivity. *J. Org. Chem.* **2014,** *79,* 10081-10093.

43. Lamport, Z. A.; Haneef, H. F.; Anand, S.; Waldrip, M.; Jurchescu, O. D. Tutorial: Organic Field-Effect Transistors: Materials, Structure and Operation. *J. Appl. Phys.* **2018,** *124,* 071101.

44. Umezawa, N.; Tanaka, K.; Urano, Y.; Kikuchi, K.; Higuchi, T.; Nagano, T. Novel Fluorescent Probes for Singlet Oxygen. *Angew. Chem. Int. Ed.* **1999,** *38,* 2899-2901.

45. Zhang, J.; Sarrafpour, S.; Haas, T. E.; Müller, P.; Thomas, S. W. Structure, Photophysics, and Photooxidation of Crowded Diethynyltetracenes. *J. Mater. Chem.* **2012,** *22,* 6182-6189.

46. Barlier, V. S.; Schlenker, C. W.; Chin, S. W.; Thompson, M. E. Acetylide-Bridged Tetracene Dimers. *Chem. Commun.* **2011,** *47,* 3754-3756.

47. Toyota, S.; Karashima, S.; Iwanaga, T. Synthesis and Properties of Extended π-Conjugated Compounds with 9,10-Bis(Phenylethynyl)Anthracene Units. *Bull. Chem. Soc. Japan* **2015,** *88,* 192-199.

48. Drexhage, K. H. Fluorescence Efficiency of Laser Dyes. *J. Res. Natl. Bur. Stand. Sect. A Phys. Chem.* **1976**, *80A*, 421-428.

49. Gaussian 09, Revision D.01, M. J. Frisch, G. W. Trucks, H. B. Schlegel, G. E. Scuseria, M. A. Robb, J. R. Cheeseman, G. Scalmani, V. Barone, G. A. Petersson, H. Nakatsuji, X. Li, M. Caricato, A. Marenich, J. Bloino, B. G. Janesko, R. Gomperts, B. Mennucci, H. P. Hratchian, J. V. Ortiz, A. F. Izmaylov, J. L. Sonnenberg, D. Williams-Young, F. Ding, F. Lipparini, F. Egidi, J. Goings, B. Peng, A. Petrone, T. Henderson, D. Ranasinghe, V. G. Zakrzewski, J. Gao, N. Rega, G. Zheng, W. Liang, M. Hada, M. Ehara, K. Toyota, R. Fukuda, J. Hasegawa, M. Ishida, T. Nakajima, Y. Honda, O. Kitao, H. Nakai, T. Vreven, K. Throssell, J. A. Montgomery, Jr., J. E. Peralta, F. Ogliaro, M. Bearpark, J. J. Heyd, E. Brothers, K. N. Kudin, V. N. Staroverov, T. Keith, R. Kobayashi, J. Normand, K. Raghavachari, A. Rendell, J. C. Burant, S. S. Iyengar, J. Tomasi, M. Cossi, J. M. Millam, M. Klene, C. Adamo, R. Cammi, J. W. Ochterski, R. L. Martin, K. Morokuma, O. Farkas, J. B. Foresman, and D. J. Fox, Gaussian, Inc., Wallingford CT, 2016

50. de Boer, B.; Hadipour, A.; Mandoc, M. M.; van Woudenbergh, T.; Blom, P. W. M. Tuning of Metal Work Functions with Self-Assembled Monolayers. *Adv. Mater.* **2005,** *17,* 621-625.

51. Goetz, K. P.; Li, Z.; Ward, J. W.; Bougher, C.; Rivnay, J.; Smith, J.; Conrad, B. R.; Parkin, S. R.; Anthopoulos, T. D.; Salleo, A.; Anthony, J. E.; Jurchescu, O. D. Effect of Acene Length on Electronic Properties in 5-, 6-, and 7-Ringed Heteroacenes. *Adv. Mater.* **2011,** *23,* 3698-3703.

52. Chen, J.; Martin, D. C.; Anthony, J. E. Morphology and Molecular Orientation of Thin-Film Bis(triisopropylsilylethynyl) Pentacene. *J. Mater. Res.* **2007,** *22,* 1701-1709.

53. Iwanaga, T.; Yamamoto, Y.; Nishioka, K.; Toyota, S. Efficient Synthesis and Electronic Spectra of Unsymmetrical 5,12-Diethynyltetracene Derivatives. *Synthesis* **2015**, *47*, 3997–4007.

54. Urushibara, K.; Yamada, T.; Yokoyama, A.; Mori, H.; Masu, H.; Azumaya, I.; Kagechika, H.; Yokozawa, T.; Tanatani, A. Development of Helical Aromatic Amide Foldamers with a Diphenylacetylene Backbone. *J. Org. Chem.* **2020**, *85,* 2019–2039.

55. Nesterov, E. E.; Zhu, Z.; Swager, T. M. Conjugation Enhancement of Intramolecular Exciton Migration in Poly(p-phenylene ethynylene)s. *J. Am. Chem. Soc.* **2005**, *127*, 10083–10088.

56. De Montigny, F.; Argouarch, G.; Lapinte, C. New Route to Unsymmetrical 9,10-Disubstituted Ethynylanthracene Derivatives. *Synthesis* **2006**, 293–298.

TOC GRAPHIC